

# Contact Angle Interpretation: Combining Rule for Solid–Liquid Intermolecular Potential

Daniel Y. Kwok\* and A. Wilhelm Neumann†

Department of Chemical Engineering, Massachusetts Institute of Technology, 77 Massachusetts Avenue, Cambridge, Massachusetts 02139, and Department of Mechanical and Industrial Engineering, University of Toronto, 5 King's College Road, Toronto, Ontario M5S 3G8, Canada

Received: July 21, 1999; In Final Form: October 27, 1999

Recent contact angle studies provide an experimental foundation for theoretical developments of molecular interactions. These newly obtained contact angles are interpreted in terms of combining rules for solid–liquid intermolecular potential. Results suggest that existing combining rules do not describe adequately the experimental adhesion patterns—the calculated and experimental patterns differ considerably. It is shown that the combining rule originally proposed by Hudson and McCoubrey can be improved to advance our understanding for solid–liquid interactions from like pairs. Macroscopic contact angle measurements are used to infer relationships of unlike solid–liquid interactions at a molecular level. The resulting combining rule gives a good fit to experimental adhesion and contact angle patterns for the range studied. The thermodynamic property solid surface tension can also be obtained from this relation.

## 1. Introduction

In the theory of molecular interactions and the theory of mixtures, combining rules are used to evaluate the parameters of unlike-pair interactions in terms of those of the like interactions.<sup>1–10</sup> As with many other combining rules, the Berthelot rule<sup>11</sup>

$$\epsilon_{ij} = \sqrt{\epsilon_{ii}\epsilon_{jj}} \quad (1)$$

is a useful approximation, but does not provide a secure basis for the understanding of unlike-pair interactions;  $\epsilon_{ij}$  is the potential energy parameter (well depth) of unlike-pair interactions;  $\epsilon_{ii}$  and  $\epsilon_{jj}$  are for like-pair interactions.

From the London theory of dispersion forces, the attraction potential  $\phi_{ij}$  between a pair of unlike molecules  $i$  and  $j$  is given by

$$\phi_{ij} = -\frac{3}{2} \frac{I_i I_j}{I_i + I_j} \frac{\alpha_i \alpha_j}{r_{ij}^6} \quad (2)$$

where  $I$  is the ionization potential and  $\alpha$  the polarizability. For like molecules this term becomes

$$\phi_i = -\frac{3}{4} \frac{I_i \alpha_i^2}{r_i^6} \quad (3)$$

The total intermolecular potential  $V(r_i)$  expressed by the (12:6) Lennard–Jones potential is in the form

$$V(r_i) = 4\epsilon_{ii}((\sigma_i/r_i)^{12} - (\sigma_i/r_i)^6) \quad (4)$$

where  $\sigma$  is the collision diameter. The attractive potentials in eqs 3 and 4 can be equated to give

$$\frac{3}{4} I_i \alpha_i^2 = 4\epsilon_{ii} \sigma_i^6 \quad (5)$$

Equation 5 can be used to derive  $\alpha_i$  and  $\alpha_j$ ; substituting these quantities into eq 2, we obtain

$$\phi_{ij} = -\frac{2\sqrt{I_i I_j}}{I_i + I_j} \frac{4\sigma_i^3 \sigma_j^3}{r_{ij}^6} \sqrt{\epsilon_{ii}\epsilon_{jj}} \quad (6)$$

If we write  $\phi_{ij}$  in the form  $-4\epsilon_{ij}\sigma_{ij}^6/r_{ij}^6$  such that  $\sigma_{ij} = 1/2(\sigma_i + \sigma_j)$ , the energy parameter for two unlike molecules can be expressed as

$$\epsilon_{ij} = \left( \frac{2\sqrt{I_i I_j}}{I_i + I_j} \right) \left( \frac{4\sigma_i \sigma_j}{(1 + \sigma_i/\sigma_j)^2} \right)^3 \sqrt{\epsilon_{ii}\epsilon_{jj}} \quad (7)$$

This forms the basis of the so-called combining rules for intermolecular potential. The above expression for  $\epsilon_{ij}$  can be simplified: when  $I_i = I_j$ , the first term of eq 7 becomes unity; when  $\sigma_i = \sigma_j$ , the second factor becomes unity. When both conditions are met, we obtain the well-known Berthelot rule, i.e., eq 1.

For the interactions between two very dissimilar types of molecules or materials where there is an apparent difference between  $\epsilon_{ii}$  and  $\epsilon_{jj}$ , it is clear that the Berthelot rule cannot describe the behavior adequately. It has been demonstrated<sup>12,13</sup> that the Berthelot geometric mean combining rule generally overestimates the strength of the unlike-pair interactions, i.e., the geometric mean value is too large an estimate. In general, the differences in the ionization potential are not large, i.e.,  $I_i \approx I_j$ ; thus the most serious error comes from the difference in the collision diameters  $\sigma$  for unlike molecular interactions.

For solid–liquid systems in general, the minimum of the solid–liquid interaction potential  $\epsilon_{sl}$  is often expressed in the

\* Author to whom correspondence should be addressed at Massachusetts Institute of Technology. Phone: (617) 253-6482. Fax: (617) 258-5042. E-mail: dykwok@mit.edu.

† University of Toronto. E-mail: neumann@mie.utoronto.ca.

following manner:<sup>1,4,6</sup>

$$\epsilon_{sl} = g(\sigma_l/\sigma_s)\sqrt{\epsilon_{ss}\epsilon_{ll}} \quad (8)$$

where  $g$  is a function of  $\sigma_l$  and  $\sigma_s$ ; they are, respectively, the collision diameters for the liquid and solid molecules;  $\epsilon_{ss}$  and  $\epsilon_{ll}$  are, respectively, the minima in the solid–solid and liquid–liquid potentials. Several other forms for the explicit function of  $g(\sigma_l/\sigma_s)$  have been suggested. For example, by comparing  $\epsilon_{sl}$  with the minimum in the (9:3) Lennard–Jones potential, one obtains

$$g(\sigma_l/\sigma_s) = \frac{1}{8}\left(1 + \frac{\sigma_l}{\sigma_s}\right)^3 \quad (9)$$

An alternative form has been investigated by Steele<sup>14</sup> and others:<sup>15</sup>

$$g(\sigma_l/\sigma_s) = \frac{1}{4}\left(1 + \frac{\sigma_l}{\sigma_s}\right)^2 \quad (10)$$

Obviously from the (12:6) Lennard–Jones potential, eq 7 implies

$$g(\sigma_l/\sigma_s) = \left(\frac{4\sigma_l/\sigma_s}{(1 + \sigma_l/\sigma_s)^2}\right)^3 \quad (11)$$

These are various attempts for a better representation of solid–liquid interactions from solid–solid and liquid–liquid interactions. In general, these functions are normalized such that  $g(\sigma_l/\sigma_s) = 1$  when  $\sigma_l = \sigma_s$ ; they revert to the Berthelot geometric mean combining rule eq 1 for  $g(\sigma_l/\sigma_s) = 1$ .

Nevertheless, adequate representation of unlike solid–liquid interactions from like pairs is rare; moreover, the validity of the existing combining rules for solid–liquid systems lacks experimental support. This is due to the difficulties involved in estimating the operative solid–liquid interactions. One attractive alternative is by means of the thermodynamic free energy of adhesion via wetting, as recently suggested.<sup>16–18</sup> This can be accomplished only when a set of thermodynamically significant contact angles is generated. Recent work<sup>19–21</sup> in systematic contact angle studies sheds light on this matter. Our aim is to test existing combining rules for solid–liquid intermolecular potential and, as a second objective, to construct similar ones using experimental data.

## 2. Theory

Thermodynamically, a relation of the free energy of adhesion per unit area of a solid–liquid pair is equal to the work required to separate unit area of the solid–liquid interface:<sup>22</sup>

$$W_{sl} = \gamma_{lv} + \gamma_{sv} - \gamma_{sl} \quad (12)$$

Because the free energy is directly proportional to the energy parameter,<sup>23,24</sup> i.e.,  $W \propto \epsilon$ , the Berthelot geometric mean combining rule (eq 1) for the free energy of adhesion  $W_{sl}$  can be approximated in terms of the free energy of cohesion of the solid  $W_{ss}$  and that of the liquid  $W_{ll}$ :<sup>11,23–25</sup>

$$W_{sl} = \sqrt{W_{ll}W_{ss}} \quad (13)$$

By the definitions  $W_{ll} = 2\gamma_{lv}$  and  $W_{ss} = 2\gamma_{sv}$ , eq 13 becomes

$$W_{sl} = 2\sqrt{\gamma_{lv}\gamma_{sv}} \quad (14)$$

Similarly, eq 8 can be expressed as

$$W_{sl} = 2g(\sigma_l/\sigma_s)\sqrt{\gamma_{lv}\gamma_{sv}} \quad (15)$$

Since  $W \propto \epsilon \propto \gamma \propto \sigma^{-3}$ ,<sup>6</sup> the function  $g$  can be rewritten in terms of  $\gamma_{sv}$  and  $\gamma_{lv}$  explicitly:

$$g(\sigma_l/\sigma_s) = g(\gamma_{sv}^{1/3}/\gamma_{lv}^{1/3}) \quad (16)$$

Thus, inserting eqs 9–11 into eq 15 yields, respectively, the following expressions:

$$W_{sl} = \frac{1}{4}\left(1 + \left(\frac{\gamma_{sv}}{\gamma_{lv}}\right)^{1/3}\right)^3 \sqrt{\gamma_{lv}\gamma_{sv}} \quad (17)$$

$$W_{sl} = \frac{1}{2}\left(1 + \left(\frac{\gamma_{sv}}{\gamma_{lv}}\right)^{1/3}\right)^2 \sqrt{\gamma_{lv}\gamma_{sv}} \quad (18)$$

and

$$W_{sl} = 2\left(\frac{4(\gamma_{sv}/\gamma_{lv})^{1/3}}{(1 + (\gamma_{sv}/\gamma_{lv})^{1/3})^2}\right)^3 \sqrt{\gamma_{lv}\gamma_{sv}} \quad (19)$$

Since  $W_{sl}$  now relates explicitly to  $\gamma_{lv}$  and  $\gamma_{sv}$ , the effect of changing  $\gamma_{lv}$  on  $W_{sl}$  can be examined for constant  $\gamma_{sv}$ .

Experimentally, one can in principle obtain the free energy of adhesion  $W_{sl}$  via contact angles through the Young equation:

$$\gamma_{lv} \cos \theta_Y = \gamma_{sv} - \gamma_{sl} \quad (20)$$

where  $\theta_Y$  is the Young contact angle, i.e., a contact angle that can be used in connection with the Young equation. Combining eq 20 with 12 yields a relation of  $W_{sl}$  as a function of  $\gamma_{lv}$  and  $\theta_Y$ :

$$W_{sl} = \gamma_{lv}(1 + \cos \theta_Y) \quad (21)$$

Thus, experimental results can be compared with those predicted from eqs 14, 17–19; i.e., contact angles of different liquids on one and the same solid surface can be employed to study the systematic effect of changing  $\gamma_{lv}$  on  $W_{sl}$  through  $\theta_Y$ .

We wish to point out that this strategy is straightforward; the underlying assumptions are however not trivial.<sup>16,17,26</sup> For example, there exist many metastable contact angles which are not equal to the one given by Young's equation, i.e.,  $\theta_Y$ : the contact angle made by an advancing liquid ( $\theta_a$ ) and that made by a receding liquid ( $\theta_r$ ) are not identical. The difference between  $\theta_a$  and  $\theta_r$  is called contact angle hysteresis. Contact angle hysteresis can be due to roughness and heterogeneity of a solid surface. If roughness is the primary cause, then the measured contact angles are meaningless in terms of the Young equation.

(1) On ideal solid surfaces, there is no contact angle hysteresis, and the experimentally observed contact angle is equal to  $\theta_Y$ .

(2) On smooth, but chemically heterogeneous solid surfaces,  $\theta$  is not necessarily equal to the thermodynamic equilibrium angle; nevertheless, the experimental advancing contact angle  $\theta_a$  can be expected to be a good approximation of  $\theta_Y$ . This has been illustrated using a model of heterogeneous (smooth) vertical strip surfaces.<sup>27,28</sup> Therefore, care must be exercised to ensure that the experimental apparent contact angle,  $\theta$ , is the advancing contact angle in order to be inserted into the Young equation.

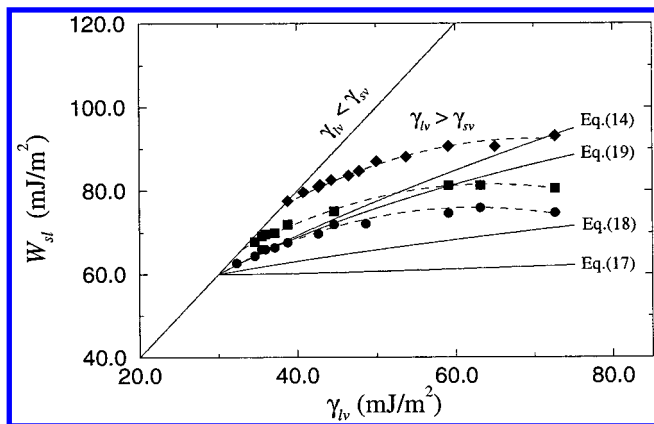


**Figure 1.** The free energy of adhesion  $W_{sl}$  vs  $\gamma_{lv}$  for polystyrene (PS) (circles), poly(styrene/methyl methacrylate, 70/30) P(S/MMA, 70/30) (squares), and poly(methyl methacrylate) PMMA (diamonds). The diagonal line is the line of zero contact angle, i.e.,  $W_{sl} = 2\gamma_{lv}$ ; other solid lines are the  $W_{sl}$  values predicted by eqs 14, 17–19 using  $\gamma_{sv} = 30$  mJ/m<sup>2</sup> from  $\gamma_{lv} = 30$  to 75 mJ/m<sup>2</sup>.

(3) On rough solid surfaces, no such equality between advancing contact angle and  $\theta_Y$  exists. Thus, all contact angles on rough surfaces are meaningless in terms of the Young equation. While the receding angle on a heterogeneous and smooth surface can also be a Young angle, it is usually found to be nonreproducible often because of sorption of the liquid into the solid and swelling of the solid by the liquid.<sup>29</sup>

The thermodynamic equilibrium angles on rough and heterogeneous surfaces are the so-called Wenzel<sup>30</sup> and Cassie<sup>31–33</sup> angles, respectively. They are not equal to  $\theta_Y$ ; furthermore, they are not experimentally accessible quantities.

Experimentally, one measures contact angles of different liquids on one and the same solid surface to fulfill the requirement of constant  $\gamma_{sv}$  for changing  $\gamma_{lv}$ . However, recent work suggested that contacting liquids often interact with the solid surface of interest in an unpredictable manner that can cause the operative  $\gamma_{lv}$ ,  $\gamma_{sv}$  (and  $\gamma_{sl}$ ) to be different from the original, anticipated one.<sup>34,35</sup> The applicability of the Young equation<sup>20</sup> is not guaranteed in such situations. Thus, experimental determination of meaningful contact angles requires painstaking efforts. A detailed discussion of these matters is available.<sup>16,17</sup>

### 3. Results and Discussion

Figure 1 displays the free energy of adhesion  $W_{sl}$  vs the liquid–vapor surface tension  $\gamma_{lv}$  from recent experimental contact angles for polystyrene (PS),<sup>19</sup> poly(styrene/methyl methacrylate, 70/30) P(S/MMA, 70/30),<sup>20</sup> and poly(methyl methacrylate) PMMA;<sup>21</sup> eq 21 was used to relate  $\theta$  to  $W_{sl}$ . The predicted patterns from eqs 14, 17–19 for a hypothetical solid surface with  $\gamma_{sv} = 30$  mJ/m<sup>2</sup> are also given. These results suggest that the above combining rules do not predict the observed adhesion patterns adequately; eqs 14 and 17 being the poorest. It should be noted that such failure is not surprising since the London dispersion theory together with the Lennard–Jones potential are only approximation and cannot account for all solid–liquid interactions.

**3.1. Improved Combining Rule.** Nevertheless, closer scrutiny suggests that the forms of the combining rules in eqs 18 and 19 may be useful in predicting the experimental adhesion patterns. As a step toward such an investigation, we rewrite

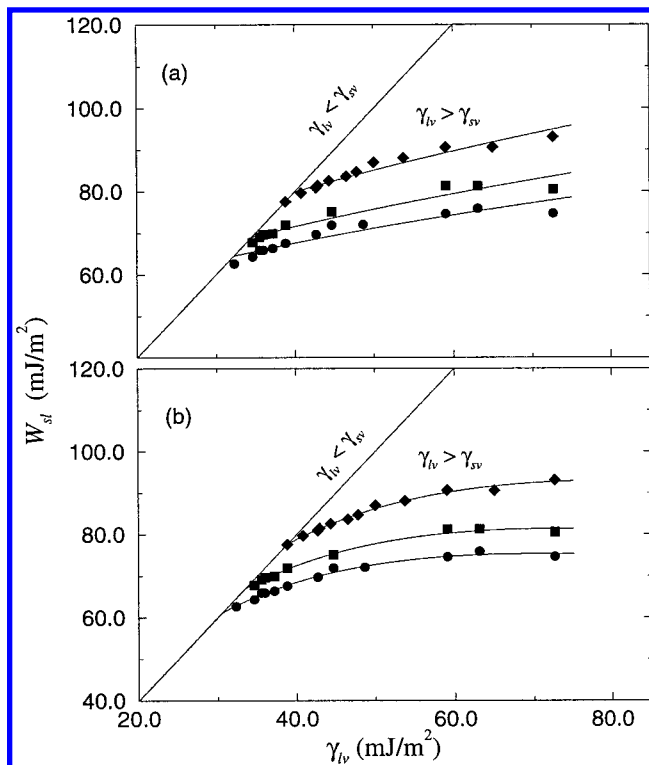


**Figure 2.** The fitted free energy of adhesion  $W_{sl}$  vs  $\gamma_{lv}$  for (a) eq 22 and (b) eq 23, for the data in Figure 1: polystyrene (PS) (circles), poly(styrene/methyl methacrylate, 70/30) P(S/MMA, 70/30) (squares), and poly(methyl methacrylate) PMMA (diamonds).

**TABLE 1: Fitting Results of Experimental Free Energy of Adhesion from Contact Angles for Equations 22 and 23**

solid surface	eq 22		eq 23	
	$\gamma_{sv}$ (mJ/m <sup>2</sup> )	$k$	$\gamma_{sv}$ (mJ/m <sup>2</sup> )	$n$
poly(methyl methacrylate), PMMA	39.9	1.3	38.9	12.6
poly(styrene/methyl methacrylate, 70/30), P(S/MMA, 70/30)	34.5	1.6	33.5	11.7
polystyrene, PS	32.3	1.7	30.6	10.9

these equations in the following generalized forms:

$$W_{sl} = 2^{1-k} \left( 1 + \left( \frac{\gamma_{sv}}{\gamma_{lv}} \right)^{1/3} \right)^k \sqrt{\gamma_{lv} \gamma_{sv}} \quad (22)$$

and

$$W_{sl} = 2 \left( \frac{4(\gamma_{sv}/\gamma_{lv})^{1/3}}{(1 + (\gamma_{sv}/\gamma_{lv})^{1/3})^2} \right)^n \sqrt{\gamma_{lv} \gamma_{sv}} \quad (23)$$

where  $k$  and  $n$  are constants to be determined. For  $k = 2$  and  $n = 3$ , eqs 22 and 23 revert respectively to eqs 18 and 19. The question now becomes how well these equations fit the experimental data in Figure 1. Assuming  $\gamma_{sv}$  to be constant for one and the same solid surface, experimental contact angle data can be used to fit these equations using a least-squares scheme.

The best-fits of eqs 22 and 23 to data are shown in Figure 2, parts a and b, respectively. Clearly, eq 23 gives a better fit to the experimental data than eq 22. The fitting results are summarized in Table 1. Although eq 23 appears to fit the data well, there is some indication that  $n$  may change with the solid surface tension  $\gamma_{sv}$ . To account for this, we assume  $n \propto \sigma_s$  (i.e.,  $n \propto \gamma_{sv}^{1/3}$ ) and square it with an as yet undetermined constant  $\alpha$

**TABLE 2: Fitting Results of Experimental Free Energy of Adhesion from Contact Angles for Equation 24**

solid surface	eq 24	
	$\gamma_{sv}$ (mJ/m <sup>2</sup> )	$\alpha$ (m <sup>2</sup> /mJ)
poly(methyl methacrylate) PMMA	38.9	1.15
poly(styrene/methyl methacrylate, 70/30) P(S/MMA, 70/30)	33.6	1.19
polystyrene PS	30.6	1.17

in the exponential, so that

$$W_{sl} = 2 \left( \frac{(\gamma_{sv}/\gamma_{lv})^{1/3}}{(1 + (\gamma_{sv}/\gamma_{lv})^{1/3})^2} \right)^{(\alpha\gamma_{sv})^{2/3}} \sqrt{\gamma_{lv}\gamma_{sv}} \quad (24)$$

Assuming  $\gamma_{sv}$  and  $\alpha$  to be constant for one and the same solid surface, we fitted the data to eq 24; the resulting  $\gamma_{sv}$  and  $\alpha$  values are summarized in Table 2. It appears that such a modification yields  $\alpha$  values that are essentially independent of the solid surfaces used. Averaging and weighting  $\alpha$  over the number of data used yields  $\alpha = 1.17$  m<sup>2</sup>/mJ. This procedure allows the determination of a combining rule for molecular potential from macroscopic contact angle measurements. Since  $\gamma_{sv} \approx K/\sigma_s^3$  and because of eq 24, the solid–liquid interaction potential  $\epsilon_{sl}$  can be expressed as

$$\epsilon_{sl} = \left( \frac{4(\sigma_l/\sigma_s)^{1/3}}{(1 + (\sigma_l/\sigma_s)^{1/3})^2} \right)^{(\alpha K/\sigma_s^3)^{2/3}} \sqrt{\epsilon_{ll}\epsilon_{ss}} \quad (25)$$

where  $\alpha$  is 1.17 m<sup>2</sup>/mJ;  $K$  is in general a constant that depends on the Boltzmann constant, absolute and critical temperatures. Such a relation can be used to estimate  $\epsilon_{sl}$  from solid–solid and liquid–liquid pairs for intermolecular potential;  $\epsilon_{sl}$  can be related directly to  $\epsilon_{ll}$  and  $\epsilon_{ss}$  by the collision diameters of the solid  $\sigma_s$  and liquid  $\sigma_l$ , as given by eq 25. In essence,  $\alpha$  replaces a constant similar to that from molecular theory. The sensitivity of  $\alpha$  relies on the validity of the assumption that the differences in the ionization potential between the liquids and solids are not large, i.e.,  $I_s \approx I_l$ ; if the difference is large, the explicit effects of  $I_l$  and  $I_s$  on  $\epsilon_{sl}$  would have to be considered in eq 25. Obviously, if further refinement of the Lennard–Jones potential is available, the above procedures together with the contact angle data can be employed to yield a more exact relation.

**3.2. Predictive Power. Free Energy of Adhesion.** Equation 24 can be used to predict the free energy of adhesion for different solid–liquid interactions. Experimental  $W_{sl}$  values from contact angles are plotted in Figure 3, for other solid surfaces not used to determine the above  $\alpha$ : these surfaces are FC722 coated-fluorocarbons,<sup>36</sup> Teflon (FEP),<sup>37</sup> poly(*n*-butyl methacrylate) (PnBMA),<sup>38,39</sup> poly(ethyl methacrylate) (PEMA),<sup>39,40</sup> poly(methyl methacrylate/*n*-butyl methacrylate) P(MMA/*n*BMA),<sup>39,41</sup> and poly(propene-*alt*-*N*-(*n*-propyl)maleimide) P(PPMI).<sup>34,35,39</sup> The values of  $W_{sl}$  as a function of  $\gamma_{lv}$  predicted by eq 24 are shown in Figure 3; each curve represents a single  $\gamma_{sv}$  value with  $\alpha = 1.17$  m<sup>2</sup>/mJ. The agreement between the predicted and experimental results is striking. From experimental contact angles on the three solid surfaces not used in Figure 3, eq 24 with  $\alpha = 1.17$  m<sup>2</sup>/mJ can be used to predict the adhesion behavior for other polar and nonpolar solid–liquid combinations.

**Contact Angles.** Contact angle patterns can also be predicted: Combining eq 24 with eq 12, we can write the solid–

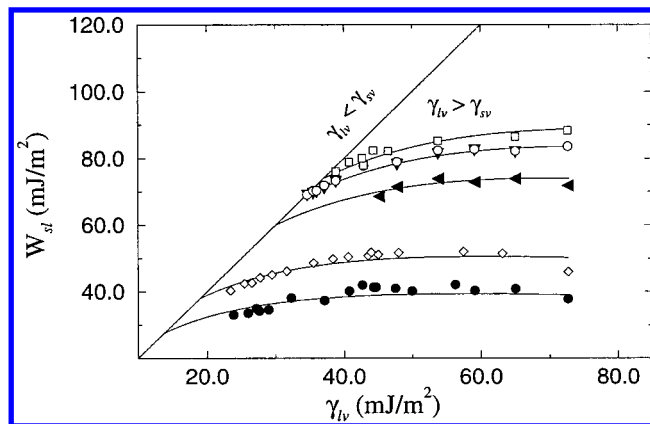


**Figure 3.** The predicted free energy of adhesion  $W_{sl}$  vs  $\gamma_{lv}$  from eq 24 with  $\alpha = 1.17$  m<sup>2</sup>/mJ for FC722 fluorocarbon-coated surface (solid circles); Teflon (FEP) (open diamonds); poly(*n*-butyl methacrylate) (PnBMA) (solid left triangles); poly(ethyl methacrylate) (PEMA) (solid down triangles); poly(methyl methacrylate/*n*-butyl methacrylate) P(MMA/*n*BMA) (open circles); poly(propene-*alt*-*N*-(*n*-propyl)maleimide) P(PPMI) (open rectangles).

liquid interfacial tension  $\gamma_{sl}$  as

$$\gamma_{sl} = \gamma_{lv} + \gamma_{sv} - 2\sqrt{\gamma_{sv}\gamma_{lv}} \left( \frac{4(\gamma_{sv}/\gamma_{lv})^{1/3}}{(1 + (\gamma_{sv}/\gamma_{lv})^{1/3})^2} \right)^{(\alpha\gamma_{sv})^{2/3}} \quad (26)$$

Thus, the Young equation (eq 20) in conjunction with eq 26 yields

$$\cos \theta_Y = -1 + 2\sqrt{\frac{\gamma_{sv}}{\gamma_{lv}}} \left( \frac{4(\gamma_{sv}/\gamma_{lv})^{1/3}}{(1 + (\gamma_{sv}/\gamma_{lv})^{1/3})^2} \right)^{(\alpha\gamma_{sv})^{2/3}} \quad (27)$$

The predicted contact angle patterns are shown in Figure 4 for  $\gamma_{sv}$  in the range from 12 to 38 mJ/m<sup>2</sup> in 2 mJ/m<sup>2</sup> increments, in plots of  $\gamma_{lv} \cos \theta$  vs  $\gamma_{lv}$  and  $\cos \theta$  vs  $\gamma_{lv}$ . These are experimental contact angles not used to obtain the values of  $\alpha$  previously. The predicted and experimental contact angle patterns agree well within  $\gamma_{sv} = \pm 1$  mJ/m<sup>2</sup>. Conversely, hypothetical contact angle values can be generated using any given pair of  $\gamma_{lv}$  and  $\gamma_{sv}$ . Using  $\gamma_{sv} = 35.0 \pm 1.0$  mJ/m<sup>2</sup> and  $\alpha = 1.17$  m<sup>2</sup>/mJ, eq 27 can predict the contact angles corresponding to each experimental  $\gamma_{lv}$  value for P(MMA/*n*BMA). The predicted angles are summarized in Table 3 together with the observed ones. The agreement is very good and within the goniometer contact angle accuracy of  $\pm 2^\circ$ .

**Solid Surface Tensions.** Further, the best-fitted experimental values (from the free energy of adhesion or contact angle patterns) to theoretical ones yield the solid surface tension  $\gamma_{sv}$ . Table 4 summarizes the fitted  $\gamma_{sv}$  values determined from eq 24 with  $\alpha = 1.17$  m<sup>2</sup>/mJ: they were obtained by using  $\gamma_{sv}$  as the only adjustable parameter to give the best fit. The fitted  $\gamma_{sv}$  values agree well with intuition that fluorocarbons should have surface tension  $\approx 12$ – $14$  mJ/m<sup>2</sup>, PS  $\approx 29$ – $31$  mJ/m<sup>2</sup>, and PMMA  $\approx 38$ – $40$  mJ/m<sup>2</sup>. We also note that the agreement with those determined from the equation of state approach for solid–liquid interfacial tensions<sup>37,42</sup> is remarkable; the results are also given in Table 4. It is apparent, and in principle obvious from fundamental considerations, that there is no conflict<sup>43</sup> between molecular theory and the equation of state approach for solid–liquid interfacial tensions; the former is based on intermolecular interactions at a molecular level; the latter on thermodynamics and macroscopic measurements. The two approaches are indeed closely related. Combining rule in intermolecular potential can

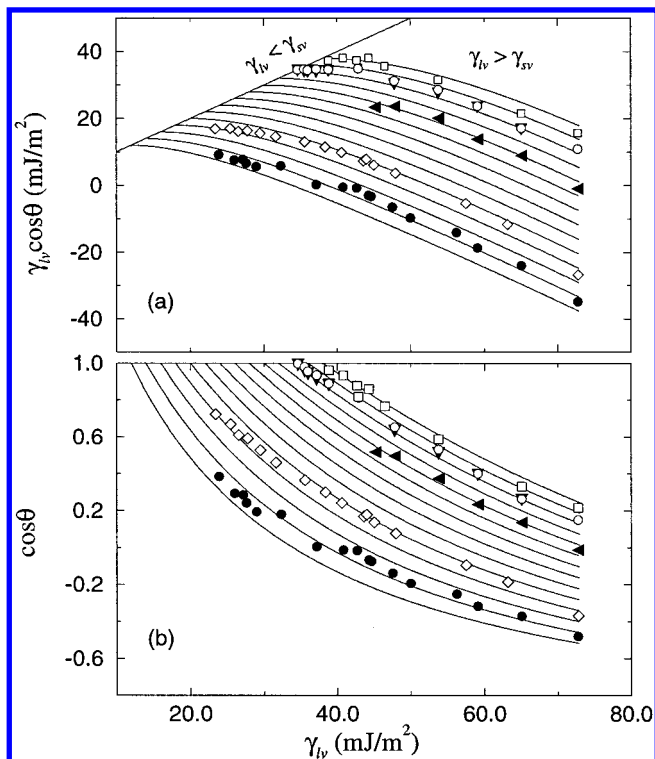


**Figure 4.** (a)  $\gamma_{lv} \cos \theta$  vs  $\gamma_{lv}$ ; (b)  $\cos \theta$  vs  $\gamma_{lv}$ . The curves were generated from eq 27 with  $\alpha = 1.17 \text{ m}^2/\text{mJ}$ , from  $\gamma_{sv} = 12$  to  $38 \text{ mJ}/\text{m}^2$  in  $2 \text{ mJ}/\text{m}^2$  increments. Each curve represents a hypothetical solid surface and hence a given  $\gamma_{sv}$ . The experimental contact angle data are same as those in Figure 3: FC722 fluorocarbon-coated surface (solid circles); Teflon (FEP) (open diamonds); poly(*n*-butyl methacrylate) (P*n*BMA) (solid left triangles); poly(ethyl methacrylate) (PEMA) (solid down triangles); poly(methyl methacrylate/*n*-butyl methacrylate) P(MMA/*n*BMA) (open circles); poly(propene-*alt*-*N*-(*n*-propyl)maleimide) P(PPMI) (open rectangles).

**TABLE 3: Comparison between the Experimental and Predicted Contact Angles for P(MMA/*n*BMA) Using Equation 27 with  $\gamma_{sv} = 35.0 \pm 1.0 \text{ mJ}/\text{m}^2$  and  $\alpha = 1.17 \text{ m}^2/\text{mJ}$**

liquid	$\gamma_{lv} \text{ (mJ/m}^2\text{)}$	$\theta \text{ (deg)}$	
		experimental	predicted
triacetin	35.52	$11.5 \pm 1.4$	$9.9 \pm 7.3$
ethyl cyanoacetate	36.01	$14.2 \pm 1.4$	$13.8 \pm 5.9$
ethyl cinnamate	37.17	$20.8 \pm 1.7$	$20.2 \pm 4.6$
methyl salicylate	38.82	$27.2 \pm 0.9$	$26.8 \pm 3.8$
1-iodonaphthalene	42.92	$35.7 \pm 0.4$	$38.6 \pm 2.9$
3-pyridylcarbinol	47.81	$49.2 \pm 0.5$	$48.9 \pm 2.2$
2,2'-thiodiethanol	53.77	$57.9 \pm 0.4$	$58.8 \pm 2.1$
formamide	59.08	$66.3 \pm 0.4$	$66.0 \pm 2.0$
glycerol	65.02	$74.7 \pm 0.6$	$73.0 \pm 1.8$
water	72.70	$81.3 \pm 0.8$	$80.6 \pm 1.6$

be used to determine solid surface tensions, just as the equation of state approach for solid–liquid interfacial tensions.

#### 4. Conclusions

We have generalized a combining rule for intermolecular potential, by modifying the original form given by Hudson and McCoubrey.<sup>3</sup> Such a relation relates the energy parameter for solid–liquid interactions  $\epsilon_{sl}$  with those of the solid–solid and liquid–liquid pairs in terms of the collision diameters. It can also be related to the free energy of adhesion and contact angles. The agreement between the predicted and experimental adhesion and contact angle patterns is remarkable, for the range studied. We have also shown that the best-fits of our equation to the

**TABLE 4: Fitting Results of the Solid Surface Tension  $\gamma_{sv}$  Using Equation 27 to Experimental Contact Angles with  $\alpha = 1.17 \text{ m}^2/\text{mJ}$ ; the Averaged  $\gamma_{sv}$  Values Determined from the Equation of State Approach from the Same Set of Data Are Given Also**

solid surface	$\gamma_{sv} \text{ (mJ/m}^2\text{)}$	
	eq 27	equation of state approach <sup>37,42</sup>
FC722	14.1	12.1
FEP	19.2	17.8
P <i>n</i> BMA	29.8	28.8
PS	30.6	30.2
P(S/MMA, 70/30)	33.5	33.2
PEMA	34.3	34.0
P(MMA/ <i>n</i> BMA)	34.8	34.6
PET	36.2	35.4
P(PPMI)	37.2	37.3
PMMA	38.9	38.7

adhesion and contact angle patterns yield the solid-surface tensions that are essentially identical to those determined from the equation of state approach for solid–liquid interfacial tensions.

**Acknowledgment.** This research was supported by the Natural Sciences and Engineering Research Council (NSERC) of Canada under Grants A8278 and EQP173469. Financial support from a NSERC Postdoctoral Fellowship (D.Y.K.) held at M.I.T. is gratefully acknowledged. D.Y.K. gratefully acknowledges Professor Paul E. Laibinis at M.I.T. for helpful discussion and financial support.

#### References and Notes

- Reed, T. M. *J. Phys. Chem.* **1955**, *59*, 425.
- Reed, T. M. *J. Phys. Chem.* **1955**, *55*, 428.
- Hudson, G. H.; McCoubrey, J. C. *Trans. Faraday Soc.* **1960**, *56*, 761.
- Fender, B. E. F.; Halsey, G. D., Jr. *J. Chem. Phys.* **1962**, *36*, 1881.
- Sullivan, D. E. *Phys. Review B* **1979**, *20* (10), 3991.
- Sullivan, D. E. *J. Chem. Phys.* **1981**, *74* (4), 2604.
- Matyushov, D. V.; Schmid, R. *J. Chem. Phys.* **1996**, *104* (21), 8627.
- Rowlinson, J. S.; Swinton, F. L. *Liquids and Liquid Mixtures*; Butterworth Scientific: London, 1981.
- Chao, K. C.; Robinson, R. L., Jr. *Equation of State: Theories and Applications*; American Chemical Society: Washington, D. C., 1986.
- Steele, W. A. *The Interaction of Gases with Solid Surfaces*; Pergamon Press: New York, 1974.
- Berthelot, D. *Compt. Rend.* **1898**, *126*, 1857.
- Israelachvili, J. N. *Proc. R. Soc. London A* **1972**, *331*, 39.
- Kestin, J.; Mason, E. A. *AIP Conf. Proc.* **1973**, *11*, 137.
- Steele, W. A. *Surf. Sci.* **1973**, *36*, 317.
- Lane, J. E.; Spurling, T. H. *Aust. J. Chem.* **1976**, *29*, 8627.
- Kwok, D. Y. *Contact Angles and Surface Energetics*. Ph.D. Thesis, University of Toronto, 1998.
- Kwok, D. Y.; Neumann, A. W. *Adv. Colloid Interface Sci.* **1999**, *81*, 167.
- Kwok, D. Y.; Neumann, A. W. *Colloids Surf., A* **1999**, *161*, 31.
- Kwok, D. Y.; Lam, C. N. C.; Li, A.; Zhu, K.; Wu, R.; Neumann, A. W. *Polym. Eng. Sci.* **1998**, *38*, 1675.
- Kwok, D. Y.; Lam, C. N. C.; Neumann, A. W. Wetting behavior and solid surface tension for a 70:30 copolymer of polystyrene and poly(methyl methacrylate). *Russ. J. Colloid Interface Sci.* **1999**, in press.
- Kwok, D. Y.; Leung, A.; Lam, C. N. C.; Li, A.; Wu, R.; Neumann, A. W. *J. Colloid Interface Sci.* **1998**, *206*, 44.
- Dupré, A. *Théorie Mécanique de la Chaleur*; Gauthier-Villars: Paris, 1969.
- Good, R. J.; Elbing, E. *Ind. Eng. Chem.* **1970**, *62* (3), 72.
- Maitland, G. C.; Rigby, M.; Smith, E. B.; Wakeham, W. A. *Intermolecular Forces: Their Origin and Determination*; Clarendon Press: Oxford, 1981.
- Girifalco, L. A.; Good, R. J. *J. Phys. Chem.* **1957**, *61*, 904.
- Kwok, D. Y.; Neumann, A. W. *Prog. Colloid Polym. Sci.* **1998**, *109*, 170.
- Neumann, A. W. *Adv. Colloid Interface Sci.* **1974**, *4*, 105.

- (28) Li, D.; Neumann, A. W. Thermodynamic status of contact angles. In Spelt, J. K., Neumann, A. W., Eds.; *Applied Surface Thermodynamics*; Marcel Dekker Inc.: New York, 1996; pp 109–168.
- (29) Sedev, R. V.; Petrov, J. G.; Neumann, A. W. *J. Colloid Interface Sci.* **1996**, *180*, 36.
- (30) Wenzel, R. N. *Ind. Eng. Chem.* **1936**, *28*, 988.
- (31) Cassie, A. B. D. *Discuss. Faraday Soc.* **1948**, *3*, 11.
- (32) Baxter, S.; Cassie, A. B. D. *J. Textile Inst.* **1945**, *36*, 67.
- (33) Cassie, A. B. T.; Baxter, S. *Trans. Faraday Soc.* **1944**, *40*, 546.
- (34) Kwok, D. Y.; Gietzelt, T.; Grundke, K.; Jacobasch, H.-J.; Neumann, A. W. *Langmuir* **1997**, *13*, 2880.
- (35) Kwok, D. Y.; Lam, C. N. C.; Li, A.; Leung, A.; Neumann, A. W. *Langmuir* **1998**, *14*, 2221.
- (36) Kwok, D. Y.; Lin, R.; Mui, M.; Neumann, A. W. *Colloids Surf., A* **1996**, *116*, 63.
- (37) Li, D.; Neumann, A. W. *J. Colloid Interface Sci.* **1992**, *148*, 190.
- (38) Kwok, D. Y.; Leung, A.; Li, A.; Lam, C. N. C.; Wu, R.; Neumann, A. W. *Colloid Polym. Sci.* **1998**, *276*, 459.
- (39) Kwok, D. Y.; Ng, H.; Neumann, A. W. Experimental study on contact angle patterns: liquid surface tensions less than solid surface tensions. *J. Colloid Interface Sci.* **1999**, in press.
- (40) Kwok, D. Y.; Wu, R.; Li, A.; Neumann, A. W. Contact angle measurements and interpretation: wetting behavior and solid surface tensions for poly(alkyl methacrylate) polymers. *J. Adhes. Sci. Technol.* **1999**, in press.
- (41) Kwok, D. Y.; Lam, C. N. C.; Li, A.; Neumann, A. W. *J. Adhes.* **1998**, *68*, 229.
- (42) Spelt, J. K.; Li, D. The equation of state approach to interfacial tensions. In Spelt, J. K., Neumann, A. W., Eds.; *Applied Surface Thermodynamics*; Marcel Dekker Inc.: New York, 1996, pp 239–292.
- (43) van Giessen, A. E.; Bukman, D. J.; Widom, B. *J. Colloid Interface Sci.* **1997**, *192*, 257.